

# Stable and unstable periodic orbits in the one dimensional lattice $\phi^4$ theory

Kenichiro Aoki\*

*\*Research and Education Center for Natural Sciences and Hiyoshi Dept. of Physics,  
Keio University, Yokohama 223-8521, Japan*

Periodic orbits for the classical  $\phi^4$  theory on the one dimensional lattice are systematically constructed by extending the normal modes of the harmonic theory, for periodic, free and fixed boundary conditions. Through the process, we investigate which normal modes of the linear theory can or can not be extended to the full non-linear theory and why. We then analyze the stability of these orbits, clarifying the link between the stability, parametric resonance and the Lyapunov spectra for these orbits. The construction of the periodic orbits and the stability analysis is applicable to theories governed by Hamiltonians with quadratic inter-site potentials and a general on-site potential. We also apply the analysis to theories with on-site potentials that have qualitatively different behavior from the  $\phi^4$  theory, with some concrete examples.

## I. INTRODUCTION

Periodic motion is truly a classic topic in classical mechanics, with the harmonic oscillator being a typical example. Periodic motions are ubiquitous in nature, and physical systems, such as a pendulum, often also contain anharmonicity at some level. Therefore, linear and non-linear oscillations have been studied for a long time[1]. For systems with many degrees of freedom, the harmonic theory is well understood and can be analyzed in terms of normal modes of the theory, by using their linear combinations. However, when the system has many continuous degrees of freedom and is anharmonic, there is still some progress to be made in the systematic study of their periodic orbits.

In this work, we systematically construct periodic orbits in non-linear lattice models by extending normal modes of the harmonic theory. The class of models we study are conservative, Hamiltonian systems, with quadratic inter-site potentials and general on-site potentials. In these models, the origin of the non-linearity is contained in the localized on-site potentials. In particular, we investigate the  $\phi^4$  theory, with periodic, fixed and free boundary conditions, in some detail. The main purpose of this work is to explicitly work out how the various aspects of the non-linear dynamics come together in generalizing the normal modes to these class of models. Through the construction of the periodic solutions in the non-linear theories, we clarify which modes in the linear theory can and can not be extended. We then analyze their stability from a dynamical systems viewpoint. In the process, we compute the Lyapunov spectra along these periodic orbits, and show quantitatively how they are related to the stable and unstable modes that appear, as the energy corresponding to the periodic orbit is changed. Furthermore, a general method of finding extensions of normal modes in lattice theories with quadratic inter-site and general on-site potentials is constructed, and explained with examples.

While the dynamics of the theories we study here are of interest on their own, these theories arise naturally as discretized versions of the continuum field theory, of which  $\phi^4$  theory is a typical case.  $\phi^4$  theory has been studied from various points of view on the lattice: Classically, the transport properties of the theory have been investigated from statistical mechanics viewpoint at finite temperatures[2, 3] and their relation to dynamical systems aspects of the theory, including the Lyapunov spectrum and dimensional loss[4], with thermostats. The on-site potentials of the models we study destroy the shift symmetry properties of the fields (cf. Sect. II) that exist in well studied models such as the FPU model[5], leading to qualitatively different dynamical behavior, such as the bulk behavior of transport coefficients[6]. The chaotic properties and the Lyapunov exponents of the non-thermostatted  $\phi^4$  theory, as well as some of its periodic orbits have also been investigated[7]. The  $\phi^4$  theory, including quantum effects, has been studied in such topics as triviality[8], and non-perturbative aspects of particle physics phenomenology[9], since the  $\phi^4$  theory is a part of the Standard Model. While the physics of the  $\phi^4$  theory investigated in this work is classical, understanding of the classical theory is also important to the understanding of the quantum theory, and furthermore, classical solutions can be an important contributing factor in quantum theories.

The periodic orbits we study are so-called “non-linear normal modes” of the class of non-linear models. Non-linear normal modes have been studied extensively for some time and various general properties have been established[10–15], and investigated in models such as the FPU model[16–18]. Most of the explicit work conducted so far seems to focus on theories with non-linear inter-site couplings. These properties can, for instance, represent non-linearity in

---

\* E-mail: ken@phys-h.keio.ac.jp.

the elastic response of materials and can be of practical importance. Accordingly, much applied research has been performed on the subject[19]. We believe that our work, which concentrates on models with quadratic inter-site potentials, with non-linear couplings that are local, contributes results complementary to the current research in the dynamics of non-linear systems with many coupled degrees of freedom.

## II. LATTICE $\phi^4$ THEORY IN ONE SPATIAL DIMENSION

Let us review the  $\phi^4$  theory on an one-dimensional lattice with  $N$  sites, in brief, partly to fix the notation. The Hamiltonian of the theory is

$$H = \sum_{j=1}^N \frac{p_j^2}{2} + \sum_{j=1}^{N-1} \frac{(q_{j+1} - q_j)^2}{2} + H_B + \sum_{j=1}^N \frac{q_j^4}{4} \quad , \quad (1)$$

where the potential terms at the ends,  $H_B$ , depend on the boundary conditions as

$$H_B = \frac{1}{2}(q_N - q_1)^2 \quad (\text{periodic bc}), \quad H_B = \frac{1}{2}(q_N^2 + q_1^2) \quad (\text{fixed bc}), \quad H_B = 0 \quad (\text{free bc}). \quad (2)$$

The non-linearity of the system is provided by the quartic on-site potential, or the tethering potential. The on-site potential destroys the shift symmetry (shifting all  $q_j$  by a constant), which exist in other well studied non-linear models such as the FPU model, leading to a different dynamical behavior for them. The system has a quartic coupling of essentially one, and is not a weakly coupled theory, in general. The equations of motion for the theory are accordingly,

$$\dot{q}_j = p_j, \quad \dot{p}_j = q_{j+1} + q_{j-1} - 2q_j - q_j^3 \quad j = 1, 2, \dots, N \quad . \quad (3)$$

The boundary conditions may be specified as,

$$q_0 = q_N, q_{N+1} = q_1 \quad (\text{periodic}), \quad q_0 = q_{N+1} = 0 \quad (\text{fixed}), \quad q_0 = q_1, q_{N+1} = q_N \quad (\text{free}) \quad . \quad (4)$$

We note the fixed boundary condition by itself also breaks the shift symmetry. The two boundaries may also have different conditions, which shall not be considered here.

## III. SYSTEMATIC CONSTRUCTION OF PERIODIC ORBITS IN $\phi^4$ THEORY

In this section, we construct a class of periodic solutions in the  $\phi^4$  theory on the lattice, based on the normal modes of the harmonic theory. A more general study of periodic solutions using powerful group theoretical methods have been conducted[15, 20, 21], and have been applied to models such as the FPU model[18]. Here, we briefly explain a more elementary approach to the solutions which hopefully provides some different insight, and derive the results needed later. The class of solutions we study are sometimes called non-linear normal modes or one dimensional bushes[15, 20, 21].

Suppose that the  $N$  linearly independent normal modes of the harmonic chain are,

$$y_j = a_j^{(m)} \cos \omega^{(m)} t, \quad m = 0, 1, \dots, N-1. \quad (5)$$

These normal modes satisfy the *linear* equations of motion,

$$\ddot{y}_j = y_{j+1} + y_{j-1} - 2y_j = \left( a_{j-1}^{(m)} + a_{j+1}^{(m)} - 2a_j^{(m)} \right) \cos \omega^{(m)} t = -(\omega^{(m)})^2 a_j^{(m)} \cos \omega^{(m)} t \quad . \quad (6)$$

The solutions to these linear equations of motion may be found using the coefficients of the form,  $a_j^{(m)} = \text{Re}(\text{const.} \times \exp(ik^{(m)}j))$ , and the harmonic frequencies can be found as,

$$\omega^{(m)} = 2 \left| \sin \frac{k^{(m)}}{2} \right| \quad , \quad (7)$$

The values of  $k^{(m)}$  depend on the boundary conditions.

We shall analyze which of these solutions extend to the  $\phi^4$  theory, for *general*  $N$ . Specifically, we look for solutions of the non-linear theory, in which all the coordinates undergo the same motion, except possibly the amplitudes of the motion. Using the ansatz,

$$q_j = a_j^{(m)} f^{(m)}(t) \quad , \quad (8)$$

the equations of motion reduce to

$$a_j^{(m)} \ddot{f}^{(m)}(t) = -(\omega^{(m)})^2 a_j^{(m)} f^{(m)}(t) - (a_j^{(m)})^3 (f^{(m)}(t))^3 \quad . \quad (9)$$

These equations are consistent if and only if the non-trivial equations are independent of  $j$ . This is satisfied when the square of non-zero coefficients,  $a_j^{(m)}$ , are independent of  $j$ ,

$$(a_j^{(m)})^2 = C \quad \text{when} \quad a_j^{(m)} \neq 0 \quad , \quad (10)$$

in which case, the equations of motion reduce to an ordinary differential equation for a non-linear oscillator,  $z(t) = a_j^{(m)} f^{(m)}(t)$

$$\ddot{z} = -(\omega^{(m)})^2 z - z^3 \quad . \quad (11)$$

The solutions to these equations are periodic in time. Though seemingly simple, the procedure has reduced the non-linear coupled  $2N$  first order differential equations to just one second order differential equation. While there seem to be a few definitions of the “non-linear normal modes”, periodic orbits constructed above are non-linear normal modes in the strict sense[10]. The motion of the coordinates are “similar” and synchronous — they all undergo identical motion with respect to time, except for their amplitudes. It is important to note that the periodic orbits we have found here exhausts all the synchronous oscillations that can have arbitrary overall amplitudes. This is because all such modes should still be synchronous when the overall amplitude goes to zero. In this limit, the dynamics become harmonic, and the motions need to reduce to the standard linear normal modes. Obviously, changing the overall amplitude of a motion is equivalent to changing its energy. The non-linearity of the theory manifests itself in the motions themselves; the shapes and the periods of the orbits depend on their energy, which is a qualitatively different behavior from the linear theory.

Clearly, this kind of construction is valid for any equations of motion, in which the couplings between the sites lead to linear terms in the equations of motion, and the only non-linearities are due to the on-site potential. In particular, this construction works for any boundary condition, since the boundary conditions change only the linear parts of the equations of motion. Another point evident in the above derivation is that this construction can be generalized to a theory with any on-site potential. We shall investigate the dynamics of on-site potentials other than the  $\phi^4$  theory in Sect. V.

Let us consider some simple examples :

*a. Symmetric orbit for periodic boundary conditions, for any  $N$*  In the harmonic theory, when the boundary condition is periodic, a trivial solution with an arbitrary shift by a constant is a solution to the equations of motion, with  $\omega^2 = 0$ . This satisfies the condition, Eq. (10), so that this solution  $q_e$ , which we shall call “symmetric” can be extended to the non-linear  $\phi^4$  theory, with the equations of motion[7]

$$\ddot{q}_e = -q_e^3 \quad . \quad (12)$$

While the original solution of the harmonic theory was just a constant shift, it should be noted that this equation is a non-linear equation and hardly trivial. This contrasts with other models with non-linearities only in the inter-site couplings, such as the FPU model. In such models, these solutions are trivial.

*b. Antisymmetric orbits for periodic boundary condition, when  $N$  is even* Without the on-site potential, the “antisymmetric” normal mode  $q_{2j} = -q_{2j+1} = q_o, p_{2j} = -p_{2j+1} = p_o$  (any  $j$ ) exists. This satisfies the condition Eq. (10) so that the equations of motion can also be extended to the  $\phi^4$  theory as[7]

$$\ddot{q}_o = -q_o^3 - 4q_o \quad . \quad (13)$$

While these constructions might seem simple, not all normal modes can be extended to the non-linear theory and the resulting equations are non-trivial. This distinction between the linear and non-linear theories is quite clear, for instance, when we consider the  $N = 3$  system with periodic boundary conditions. In this case, the three linearly independent normal modes in the harmonic theory have amplitudes of constant times  $(1, 1, 1), (1, -1, 0), (0, 1, -1)$ , for the three coordinates. All these modes can be extended to the  $\phi^4$  theory. However, a mode that can be obtained from

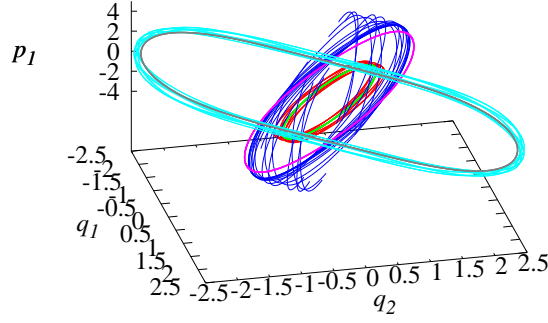


FIG. 1: Periodic orbits and their perturbations for  $N = 2$ : The symmetric trajectory for  $E/N = 8$  (brown), antisymmetric trajectories for  $E/N = 2$ (green) ,8(magenta) and their perturbations (cyan, red, blue, respectively). Antisymmetric trajectory for  $E/N = 8$  is dynamically unstable, while others are not, which is visible. All trajectories,  $(q_1, q_2, p_1)$ , were started with  $q_1 = q_2 = 0$  and were followed for the same amount of time,  $\Delta t = 40$ . Perturbed orbits were obtained by increasing the initial  $p_1$  value by 10%.

two of the modes which have the same frequency, with amplitudes,  $(2, -1, -1)$ , is also a normal mode in the harmonic theory, that can *not* be extended to the non-linear theory, since it does not satisfy the condition, Eq. (10). On the other hand, a solution that can be obtained as a sum of the amplitudes that satisfy the condition, Eq. (10), is not a simple sum of the solutions and is another non-trivially different solution in the  $\phi^4$  theory, since the equations of motion are non-linear. Some symmetric and antisymmetric orbits, along with their perturbed trajectories are shown for the  $N = 2$  lattice with periodic boundary conditions in Fig. 1.

While we mentioned some simple examples above, we list the normal modes that can be extended for the three boundary conditions, periodic, fixed and free, up to  $N = 9$  in Table I. The results depend on the boundary conditions in an interesting manner, as we explain. The general theory of these modes have been established previously[15, 20, 21], using group theoretical methods. The results in Table I were obtained by solving the condition, Eq. (10). The general case, including these, is explained below. The symmetric orbits explained above, are not shown in this table, and exists for any  $N$  when the boundary conditions are periodic or free. The modes in Table I are listed simply with the amplitudes of each  $q_j$  and this can be multiplied by any common constant value, and still be a periodic orbit. We have only listed modes which are inequivalent. In particular, the modes which are equivalent by just by shifting the oscillator in the periodic case, or by reflection (oscillator  $j \leftrightarrow N - j$ ) are not listed in the tables.

$N$	$\omega^2$	$a_j$ (periodic bc)	$N$	$\omega^2$	$a_j$ (fixed bc)	$N$	$\omega^2$	$a_j$ (free bc)
2	4	(1, -1)	2	1	(1, 1)	2	2	(1, -1)
3	3	(1, -1, 0)	3		(1, -1)	3	1	(1, 0, -1)
4	2	(1, 1, -1, -1)	3	2	(1, 0, -1)	4	2	(1, -1, -1, 1)
	2	(0, 1, 0, -1)	5	1	(1, 1, 0, -1, -1)	6	1	(1, 0, -1, -1, 0, 1)
	4	(1, -1, 1, -1)		2	(1, 0, -1, 0, 1)		2	(1, -1, -1, 1, 1, -1)
6	1	(0, 1, 1, 0, -1, -1)	3		(1, -1, 0, 1, -1)	8	2	(1, -1, -1, 1, 1, -1, -1, 1)
	3	(1, -1, 0, 1, -1, 0)	7	2	(1, 0, -1, 0, 1, 0, -1)	9	1	(1, 0, -1, -1, 0, 1, 1, 0, -1)
	4	(1, -1, 1, -1, 1, -1)	8	1	(1, 1, 0, -1, -1, 0, 1, 1)			
8	2	(1, 1, -1, -1, 1, 1, -1, -1)	3		(1, -1, 0, 1, -1, 0, 1, -1)			
	2	(0, 1, 0, -1, 0, 1, 0, -1)	9	2	(1, 0, -1, 0, 1, 0, -1, 0, 1)			
	4	(1, -1, 1, -1, 1, -1, 1, -1)						
9	3	(1, -1, 0, 1, -1, 0, 1, -1, 0)						

TABLE I: Rescaled amplitudes for the non-linear periodic modes up to  $N = 9$  for periodic (left), fixed (middle) and free (right) boundary conditions. In addition, the symmetric solutions  $a_j = 1$  (any  $j$ ) with  $\omega^2 = 0$  exist for all  $N$  in the periodic and free boundary cases, which are not shown.

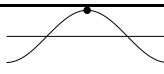
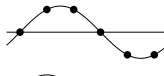


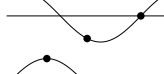
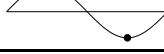
label	$\omega^2$	period	amplitudes	mode
0	0	1	(1)	
1	1	6	(0, 1, 1, 0, -1, -1)	
2a	2	4	(1, 1, -1, -1)	
2b	2	4	(0, 1, 0, -1)	
3	3	3	(1, -1, 0)	
4	4	2	(1, -1)	

TABLE II: Allowed basic modes and their rescaled amplitudes. The modes are labeled for reference (see text).

The general solution can be understood as follows: Since the coefficients for the linear equations, Eq. (6), are integers,  $(\omega^{(m)})^2$  are also integers, under the condition Eq. (10). Due to the value of these coefficients, only 0, 1, 2, 3 and 4 are possible, corresponding to the periods on the lattice of, 1, 6, 4, 3 and 2, respectively, as tabulated in Table II. To make the relationship between  $\omega^2$ , periodicity and the mode clear, a graphical representation of the basic modes are also shown. All the modes are repetitions of these modes, except close to the boundaries, as explained below. Corresponding modes have been derived for the FPU model with periodic boundary conditions[18]. While the results are similar, it is interesting to note the differences. The  $\phi^4$  theory, unlike the FPU model, contains an on-site potential that leads to *non-linear local* interactions. This enforces the non-zero amplitudes of the oscillations to be equal, as seen in Eq. (10), which is not the case for the FPU model.

Periodic boundary conditions are the simplest to understand. All the solutions are repetitions of the modes in Table II, and the condition for the non-linear periodic solutions to exist is that  $N$  is a multiple of a period in Table II.  $\omega^2$  will then have the corresponding value. All the basic modes listed in Table II are allowed. The solutions up to  $N = 9$  are listed in Table I(left) can be all understood from this logic, and in particular, only the symmetric solution exists for prime numbers  $N(> 3)$ . The symmetric mode, where all the amplitudes are the same value, exists for any  $N$ .

For fixed boundary conditions, the values at the boundaries need to be 0 as in Eq. (4), so that 0 needs to be contained in the amplitudes and only the modes 1, 2b, 3 are allowed (Table II). The periodicity of the zeros for these modes are 3, 2, 3, respectively, so that the condition for these modes to exist is that  $N + 1$  is a multiple of 2, 3 and the solutions are repetitions of the basic modes 1, 2b, 3, adjusted so that the zeros are at the boundaries. In some cases, only half of a basic mode might appear at the boundary, as in the case the first mode for  $N = 8$  and the mode for  $N = 9$  in Table I(middle). A general non-linear mode can be constructed this way, which are listed in Table I(middle), up to  $N = 9$ . While the mode (1, 1) appears for  $N = 2$ , unlike the symmetric modes for the periodic and the free boundary conditions, it is a part of mode 1 in Table II with  $\omega^2 = 1$ . For other values of  $N$ , no mode with all amplitudes being equal appears for fixed boundary conditions.

For free boundary conditions, the two consecutive sites with the same values need to appear, so that only the basic modes 0, 1, 2a in Table II are allowed. The symmetric mode (mode 0), which obviously has this property, exists for any  $N$ . The periodicity between the identical consecutive values for modes 1, 2a are 2, 3, respectively, so that the non-linear modes exist for  $N$  being multiples of 2, 3. All modes can be understood in this manner and they are listed up to  $N = 9$  in Table I(right).

#### IV. STABILITY AND INSTABILITY OF THE PERIODIC ORBITS

The periodic orbits explained in the previous section have only two first order degrees of freedom in essence, and might not seem “chaotic”. However, they can be unstable from a dynamical systems perspective. In this work, we investigate the stability, or lack thereof, of the periodic orbits, from this point of view. When the orbit is unstable, perturbations grow exponentially large with time. Therefore, this instability appears as the positive maximal Lyapunov exponent along the orbit. Obviously, the instability can also be seen explicitly by following perturbed trajectories. If the exponent is positive, a small perturbation on the orbit will cause the trajectory to diverge exponentially from the

periodic orbit. While, this tells us how to discriminate when the orbit is unstable, it does *not* tell us *why* the orbit is unstable or stable. For this, we now turn to an analysis of the perturbations around the orbit. General theory of stability analysis has been studied previously and have been performed explicitly for periodic orbits in the FPU model[15, 17, 21].

Partly to avoid confusion, it should be mentioned that even when the orbits are dynamically unstable, some orbits can be stable from a computational standpoint[7]. This is a technically interesting issue, perhaps of practical import, which we briefly explain: Any numerical computation contains round-off errors and has only a finite precision. Therefore, one might expect that following unstable orbits numerically for a long time is impossible, since any deviation will force the trajectory to diverge exponentially with time from its “true” trajectory. However, somewhat surprisingly, some periodic orbits can be followed for an arbitrarily long time. The reason for this is that their symmetry properties are preserved to the last bit in the data, with the appropriate coding and the use of compilers. For instance, in the integration of the the symmetric and antisymmetric orbits explained in previous section, the properties  $q_{2j} = \pm q_{2j+1}$  are fully preserved in the numerical integration. While it is unclear if this situation applies to all periodic orbits, it applies also to other orbits we investigate below. This property allows us to follow periodic trajectories and compute Lyapunov spectra averaged along them with precision, given enough computational time. In this work, we used the fourth order Runge-Kutta routine for integration and the method explained in [26] to compute the Lyapunov spectra.

Let us briefly summarize the properties of Lyapunov exponents, which will be of use to us[22, 23]. Lyapunov spectra have been computed in various Hamiltonian systems[23–29], including the  $\phi^4$  theory both thermostatted and not thermostatted[2, 7]. When one follows a trajectory in phase space, the neighboring trajectories can diverge from (or converge to) the original trajectory exponentially and their exponents per unit time are called Lyapunov exponents. If we consider all the possible different directions of the neighboring trajectories and average along the original trajectory, their rates of divergence or convergence from it, we obtain the Lyapunov spectrum. The systems considered in this work are all Hamiltonian systems, with the Hamiltonian having no explicit time dependence. For  $N$  pairs of coordinates and momenta,  $q_j, p_j$  ( $j = 1, 2, \dots, N$ ), there are  $2N$  Lyapunov exponents. The spectrum of exponents is made up of pairs of the form  $\pm\lambda$  ( $\lambda$ : Lyapunov exponent) and is invariant under changing the sign of all the exponents, due to the time reversal symmetry of the system. Furthermore, at least one pair of exponents is zero, since the trajectories are on a  $2N - 1$  dimensional constant energy surface. It should be noted, that in this work, we follow periodic orbits, which are localized in the phase space, and compute the Lyapunov spectra along them. So the Lyapunov spectra obtained here are different from the spectra obtained by averaging over the chaotic “sea” in the phase space[23–29].

### A. $N = 2$ system with periodic boundary conditions

The simplest case to analyze the stability of the periodic orbits is the  $N = 2$  system, since the  $N = 1$  system will only have zero Lyapunov exponents, and hence no instability, from the properties referred to above. Below, this system with periodic boundary conditions is analyzed in some detail. For  $N = 2$ , there are only the “symmetric” orbit, in which both coordinates are the same, and the “antisymmetric” orbit, in which the coordinates are  $(-1)$  times each other. These cases are instructive and enables us to clearly see the mechanism behind the instability of the orbit, or lack thereof, enabling us to extend this understanding to more general cases. The Lyapunov exponents for the periodic orbits has been computed in some cases[7]. It was found that the symmetric solutions, Eq. (12), seemed to have zero maximum Lyapunov exponent for any energy, though numerical computations can not rule out small non-zero exponents. In contrast, the antisymmetric orbits, Eq. (13), were found to be stable at low energies, becoming unstable at higher energies. This stark contrast is intriguing, but its underlying physics was unclear. We will see how this originates below.

The symmetries of the system are more conveniently viewed using the coordinates

$$\chi = \frac{1}{2}(q_1 - q_2), \quad \eta = \frac{1}{2}(q_1 + q_2) \quad . \quad (14)$$

Then, the equations of motion for the system can be reorganized into a more convenient form as

$$\ddot{\chi} = -\chi(\chi^2 + 3\eta^2) - 4\chi, \quad \ddot{\eta} = -\eta(\eta^2 + 3\chi^2) \quad . \quad (15)$$

To analyze the problem of stability, we perturb around a general classical solution,  $\chi_0, \eta_0$ , as  $\chi = \chi_0 + \chi_1, \eta = \eta_0 + \eta_1$ . Keeping only the leading order terms, we arrive at the equations for the fluctuations around the solution,

$$\ddot{\chi}_1 = -3(\chi_0^2 + \eta_0^2)\chi_1 - 4\chi_1 - 6\chi_0\eta_0\chi_1, \quad \ddot{\eta}_1 = -3(\eta_0^2 + \chi_0^2)\eta_1 - 6\chi_0\eta_0\eta_1 \quad . \quad (16)$$

### 1. Symmetric mode fluctuations

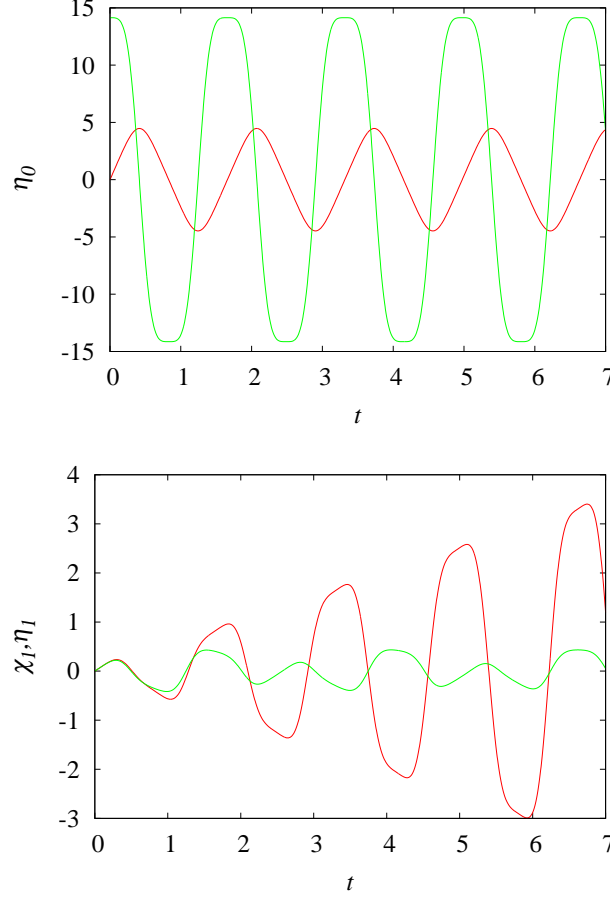


FIG. 2:  $N = 2$  symmetric orbit trajectories of  $\eta_0$  (red) and its momentum,  $\dot{\eta}_0$  (green), for  $E/N = 100$  (top figure). Time dependence of the perturbations  $\eta_1$  (red),  $\chi_1$  (green) around the symmetric mode,  $\eta_0$  (bottom figure). While  $E/N$  is relatively large, perturbation  $\eta_1$  grows only linearly with time, not exponentially, and  $\chi_1$  amplitude does not become larger.

Let us first discuss small deviations from the symmetric orbit,  $\chi_0 = 0$  and  $\eta_0$  satisfying the non-linear oscillator equation, Eq. (12). The deviations from the orbit satisfy

$$\ddot{\chi}_1 = -(3\eta_0^2 + 4)\chi_1, \quad \ddot{\eta}_1 = -3\eta_0^2\eta_1. \quad (17)$$

These equations are those of harmonic oscillators with oscillation frequencies that depend on time. The frequencies are clearly real for both equations, so that there is no trivial exponential growth. Yet  $\eta_0$  is periodic, so that solutions to these equations can exhibit parametric resonance[1], which we now investigate.

While the equations Eq. (17) can be analyzed numerically, and shall be done so below, it is worthwhile to study the mechanism analytically. Parametric resonance arises when the frequency of the oscillation changes at a rate close to twice the base frequency, to leading order. The condition for such an instability for an oscillator satisfying

$$\ddot{x} = -\omega^2(t)x = -\omega_0^2(1 + h \cos \gamma t)x, \quad (18)$$

is

$$\left| \frac{\gamma}{2\omega_0} - 1 \right| < \frac{h}{4}. \quad (19)$$

While the basic motion,  $\eta_0$  is not sinusoidal, let us approximate  $\eta_0$  by  $\sqrt{2}E_1^{1/4} \sin \Omega t$  to gain insight, where  $E_1 = E/N$  is the energy per oscillator. The frequency can be computed to be  $\Omega = (2\pi)^{3/2}E_1^{1/4}/\Gamma(1/4)^2$ . One can then show

analytically that neither  $\omega^2(t) = 3\eta_0^2$  nor  $\omega^2(t) = 3\eta_0^2 + 4$  satisfies the condition, Eq. (19), for any  $E_1$ . In particular, we note that in the first case,  $\Omega/\omega_0$  is independent of  $E_1$  and just a numerical constant. We can integrate the perturbations, Eq. (16), numerically and we find that the symmetric mode does not become unstable regardless of the energy, which is consistent with what was found analytically. An example of the perturbations is illustrated in Fig. 2. The initial conditions for the perturbations shown in the plot are chosen to be  $(\xi_1(0), \dot{\xi}_1(0)), (\eta_1(0), \dot{\eta}_1(0)) = (0, 1)$  and the same conditions will be used below for all perturbation mode analyses. The equations for the perturbations are linear with respect to  $\xi_1, \eta_1$  so that rescaling these conditions just rescales the solutions.

## 2. Antisymmetric mode fluctuations

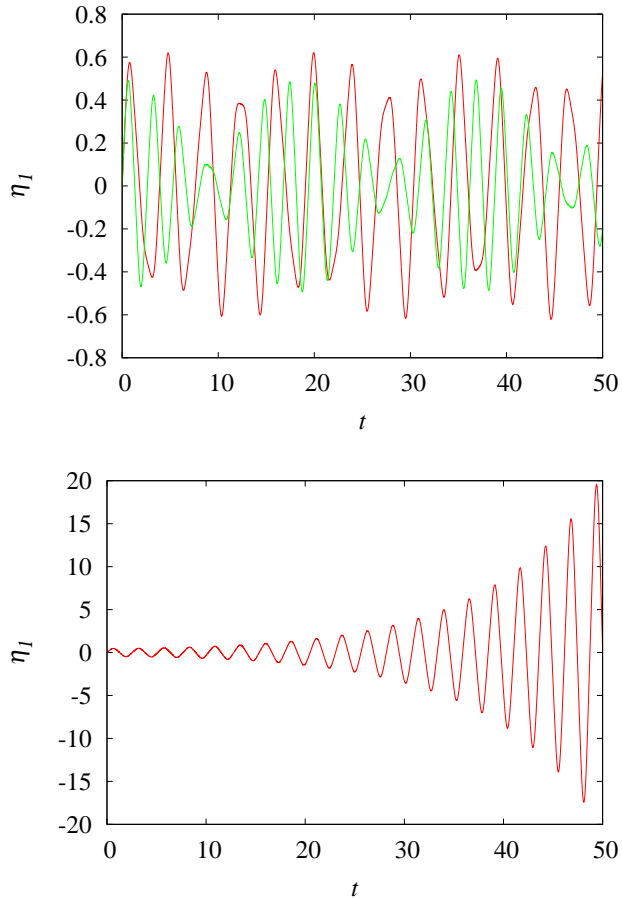


FIG. 3: Time dependence of the perturbations around the antisymmetric mode,  $\chi_0$ , for  $N = 2$ : (Top) Perturbation of  $\eta_1$  for  $E/N = 4$ (red),  $6.8$ (green). (Bottom)  $\eta_l$  for  $E/N = 7.2$ (red). The perturbations develop beat behavior and become unstable for  $E > 7.12$ .

In the antisymmetric mode,  $\eta_0 = 0$  and  $\chi_0$  satisfies the non-linear oscillator equation, Eq. (13). Similarly to the symmetric mode case, we need to consider the cases,  $\omega^2(t) = 3\chi_0^2, 3\chi_0^2 + 4$  for the equation Eq. (18). Let us keep the leading order term in  $\chi_0$  expansion and deduce what happens: Approximating  $\chi_0$  by  $\sqrt{E_1/2}\sin(2t)$ , we find that  $\omega_0^2 = 3\chi_0^2 + 4$  never satisfies the resonance condition, Eq. (19), while  $\omega_0^2 = 3\chi_0^2$  satisfies it in the region  $3.4 \simeq 2^8/(3 \cdot 5^2) < E_1 < 2^8/3^3 \simeq 9.5$ , so that there is an unstable region.

While the above analytical argument used simple crude approximations, they nevertheless give us insight as to the underlying mechanism behind the stability and instability of the perturbations. When the perturbation equations, Eq. (16), are integrated numerically, we find that indeed the mode for  $\omega^2 = 3\chi_0^2 + 4$  never becomes unstable, while that for  $\omega^2 = 3\chi_0^2$  becomes unstable for  $E/N > 7.12$ . So the analytic argument recovers the rough picture, but there is no upper bound to the energies for the instability of the perturbations around the orbits, and this is outside the



region of the validity of the analytic approximation. The transition from stable to unstable displays beat behavior just before becoming unstable, which can be seen in Fig. 3.

### B. General periodic orbits for any $N$

Let us now discuss the case for a general periodic orbit, for any  $N$  and any boundary conditions. A periodic orbit  $z_0$  satisfies the equation, Eq. (11), for some  $m_0$ , as

$$\ddot{z}_0 = - \left( \omega^{(m_0)} \right)^2 z_0 - z_0^3 . \quad (20)$$

We expand around this basic solution as  $q_j = q_{j,0} + q_{j,1}$ , where  $q_{j,0} = \pm z_0$  or 0, due to Eq. (10).

$$\ddot{q}_{j,1} = q_{j+1,1} + q_{j-1,1} - 2q_{j,1} - 3q_{j,0}^2 q_{j,1} . \quad (21)$$

These equations are linear equations with respect to  $q_{j,1}$ , but contain time dependent coefficients in  $q_{j,0}$  and furthermore,  $N$   $q_{j,1}$ 's are coupled. When the amplitudes in the mode do *not* contain zeros (*c.f.* Table I), the equations can be further simplified. In this case, using the normal mode coordinates for the perturbations,  $z_1^{(m)}$ , we obtain the form of the equations which are decoupled,

$$\ddot{z}_1^{(m)} = - \left[ \left( \omega^{(m)} \right)^2 + 3z_0^2 \right] z_1^{(m)} . \quad (22)$$

For a periodic solution of the  $\phi^4$  lattice generated by  $z_0$ ,  $N$  equations labeled by the normal mode directions,  $m$ , for the perturbations around the original periodic solution. The spectrum of the (harmonic) normal modes  $\omega^{(m)}$  enters the equation. We see that the  $N = 2$  symmetric and antisymmetric cases discussed above can be recognized as special cases of these equations. It should be noted that the unperturbed solution enters only as  $z_0$  but this exists only for certain values of  $m_0$ , as seen in Table I. The equation cleanly separates the role of the non-linear oscillatory mode in  $z_0$  and the harmonic normal modes in the spectrum,  $(\omega^{(m)})^2$ .  $N$  enters only through the spectrum.

The above second order linear differential equation, Eq. (22), with a real periodic function as the coefficient is an example of Hill's equation. Its two linearly independent solutions have one of the properties below, given by *Floquet's theorem*[30]:

- (a) The linearly independent solutions are of the form  $e^{i\alpha t} p_+(t), e^{-i\alpha t} p_-(t)$ , where,  $p_{\pm}(t)$  are periodic functions of  $t$  with the period  $T$ .
- (b) A non-trivial periodic solution,  $p(t)$  exists. Another solution,  $f(t)$  has the property  $f(t+T) = \pm f(t) + \theta p(t)$ , ( $\theta$ : constant). The period of  $p(t)$  is  $T$  or  $2T$ , and the sign in front of  $f(t)$  is  $+$  or  $-$ , respectively.

Here,  $T$  is the (minimal) period of  $z_0(t)^2$ . Exponentially growing perturbations exists if and only if the solutions are of type (a) with a non-real  $\alpha$ . Solutions of type (a) with real  $\alpha$  lead to bounded perturbations. Solutions of type (b) lead to linearly growing perturbations when  $\theta \neq 0$ .

Let us discuss here the relation between the Lyapunov exponents, perturbation equations, Eq. (22), and Floquet's theorem. Lyapunov exponents measure the exponential rate at which the deviations from a trajectory diverge from the solution. The trajectory needs not be periodic. The number of Lyapunov exponents equals the dimension of the phase space,  $2N$ , since the deviations can be made in any direction in phase space. The behavior of perturbations around a periodic solution may be obtained by solving the perturbation equations. Intuitively, it should be expected that the growth rate of the perturbations should be consistent with the Lyapunov exponents averaged along the periodic solution. This shall be quantitatively confirmed below. It should be noted that the computations involved in obtaining the Lyapunov spectra and solving the perturbation equations are quite different. To obtain the Lyapunov spectrum, in principle, we need to solve the equations of motion and measure how different solutions with close initial conditions diverge. In practice, in the method we adopt, the equations of motion for the whole system are solved while also tracking the evolution of vectors in the tangent space, a procedure that requires  $2N(N+1)$  coupled first order equations to be solved. The whole spectrum of  $2N$  exponents along with the unperturbed periodic solution is obtained this way, without using the perturbation equations, Eq. (22). On the other hand, in perturbation theory, first, the periodic solution is obtained and then, the  $N$  perturbation equations are solved, one by one. Each equation should correspond to two Lyapunov exponents. When the perturbations equation is of type (a) in Floquet's theorem and  $\alpha$  is not real, a perturbation can grow exponentially and  $\pm \text{Im } \alpha$  should coincide with the Lyapunov exponent pair  $\pm \lambda$ . In all other cases, the corresponding Lyapunov exponents are zero. This will be explicitly seen below. The pairing property is consistent with the general property of Lyapunov exponents. Interestingly, by independently solving one second order differential equation for each perturbation mode, we recover the Lyapunov exponents pair  $(\pm \lambda)$  by pair, including their degeneracies. To understand how the system works, we illustrate this with a few concrete examples.

### 1. General $N$ , symmetric solution, periodic boundary conditions

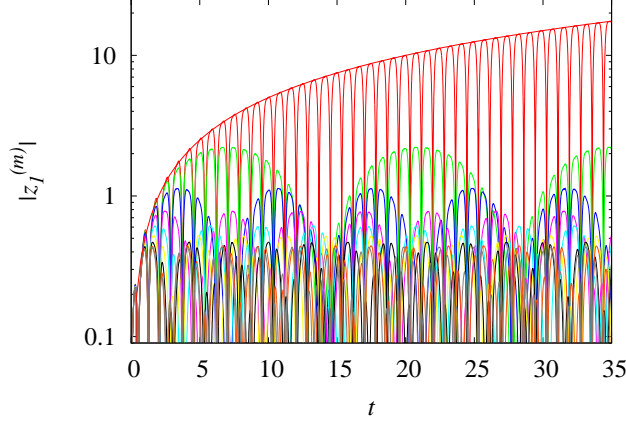


FIG. 4: Absolute values of the perturbations,  $|z_1^{(m)}|$ , ( $m = 0, 1, \dots, N/2$ ) around the symmetric solution,  $z_0^{(0)}$  as a function of time,  $t$ , for  $N = 16$ ,  $E/N = 100$ . All the different modes  $m = 0$  (red), 1(green), 2(blue), 3(magenta), 4(cyan), 5(yellow), 6(black), 7(orange),  $N/2 = 8$ (grey) are shown.  $t/2$  behavior is also shown (red), which matches well the linear, but *not* exponential, growth of  $z_1^{(0)}$ . Individual modes, apart from  $z_1^{(0)}$  are difficult to separate visually, but it can be seen that while  $E/N$  is relatively large, none of the modes have exponentially increasing amplitudes. At this  $E/N$ , the modes have decreasing amplitudes in the order,  $m = 0, 1, 2, \dots, N/2$ .

When the boundary conditions are periodic, the symmetric solution, where all coordinates and momenta move in unison,  $q_j = q_k, p_j = p_k$  (any  $j, k$ ) is a solution for general  $N$ . To analyze the perturbations to the periodic orbit through the equations, Eq. (22), we need the spectrum of the normal modes for the harmonic theory, which, for periodic boundary conditions is

$$\omega^{(m)} = 2 \sin \pi \frac{m}{N}, \quad m = 0, 1, \dots, N-1. \quad (23)$$

This spectrum is doubly degenerate except for  $m = 0$  and  $N/2$ , the latter only when  $N$  is even. So there are only  $N/2 + 1$  or  $(N + 1)/2$  independent perturbation equations, Eq. (22), depending on whether  $N$  is even or odd. When the equations Eq. (22) are integrated, we find no instabilities for small or large  $E/N$  for any  $N$ .

An example is shown in Fig. 4 for  $N = 16$  lattice at  $E/N = 100$ . While the energy of the system is relatively large, none of the perturbations grows exponentially. This result is quite consistent with the Lyapunov exponents being immeasurably small numerically, for any  $N$  and  $E/N$ [7]. In this case, the perturbations for the modes  $m = 1, 2, \dots, N/2$  belong to case (a) of Floquet's theorem, with real values of  $\alpha$ . The distinct feature of perturbations with two periods can be observed in the figure. The mode  $m = 0$  is of case (b) of Floquet's theorem with  $\theta \neq 0$ . It should be noted that  $m = 0$  coincides with the linearized normal mode of the original periodic solution, which exists for any energy. The perturbation in this direction does not grow exponentially so that the corresponding Lyapunov exponents are zero, yet grows linearly for the following reason. If  $\theta = 0$ , we would have two perturbations which are periodic when shifted with the period of the unperturbed solution  $z_0$ . This would lead to a slightly perturbed periodic solution with the same period. However, non-linear periodic solutions change both the period and the trajectory shape with the energy, which leads to a linear growth with respect to  $t$  in the perturbation. Clearly, this argument is not restricted to the symmetric periodic orbit and we shall see that this property holds for all the examples we study.

### 2. General even $N$ , antisymmetric solution, periodic boundary conditions

The situation is much more interesting for the antisymmetric periodic solution,  $q_j = -q_{j+1}, p_j = -p_{j+1}$  for general even  $N$ . When  $N = 2$ , it was seen that for large enough  $E/N$ , the orbit becomes unstable and one (of the two) fluctuation equations had a parametric resonance. For general  $N$ , there are  $N/2 + 1$  inequivalent perturbation modes, as explained above. As we increase  $E/N$ , the perturbation modes become unstable, one inequivalent mode by one. This can be seen as the solutions to the perturbation equations, Eq. (22), developing exponentially growing behavior, as in Fig. 6, which is also evidenced in the Lyapunov spectrum, Fig. 5. The number of non-zero exponents can be seen to increase systematically as  $E/N$  is increased.

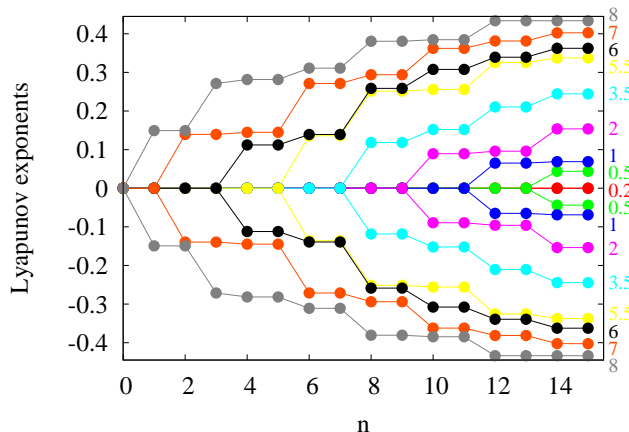


FIG. 5: Lyapunov exponents  $\{\lambda_n\}$  of  $N = 16$  antisymmetric orbits, for  $E/N = 0.2$ (red),  $0.5$ (green),  $1$ (blue),  $2$ (magenta),  $3.5$ (cyan),  $5.5$ (yellow),  $6$ (black),  $7$ (orange),  $8$ (grey) and labeled on the right hand side. The Lyapunov exponents are plotted in the increasing order of their magnitudes. The whole spectrum is always invariant under the reflection  $\lambda_n \leftrightarrow -\lambda_n$ , as it should be. More and more Lyapunov exponents are seen to become non-zero, corresponding to more perturbation modes around the periodic orbit becoming unstable. The exponents are seen to become nonzero in pairs (of  $\pm\lambda_n$  pairs) with the same values, except for  $\lambda_0 = 0$  and the last exponent to become non-zero  $\pm\lambda_3$  for  $E/N = 8$ . The exponents, including their degeneracy, reflect the properties of the perturbations.

The equations for the perturbations, Eq. (22), also reflect the degeneracy of the spectrum, Eq. (23). From the computations of Lyapunov spectra, this degeneracy is a priori not obvious, but it is indeed reflected in the Lyapunov spectra, as seen in Fig. 5. The modes become non-zero in pairs, corresponding to identical Lyapunov exponents (and  $(-1)$  times them), except for two modes, as we now explain. The two *non-degenerate* modes  $m = 0, N/2$  correspond to the symmetric and antisymmetric periodic orbits respectively. The unperturbed orbits  $z_0$  satisfy the non-linear oscillator equation Eq. (20) with  $(\omega^{(0)})^2 = 0$  or  $(\omega^{(N/2)})^2 = 4$ , neither of which depends on  $N$ . So the equations for these two perturbation modes and hence their behavior are independent of  $N$ . The mode for  $m = 0$  corresponds to a non-degenerate non-zero Lyapunov exponent pair, whose value is independent of  $N$ . This was found in [7] and the reason for this is now clear. This mode becomes unstable at the highest energy, amongst the modes.  $m = N/2$  mode direction coincides with the periodic orbit which we perturbed around, and the perturbation grows linearly for the reason explained at the end of Sect. IV B 1. In regards to Floquet's theorem, perturbation equation for  $m = N/2$  mode is of type (b) with  $\theta \neq 0$  and other modes are of type (a). In general, there needs to be a mode associated with the pair of zero Lyapunov exponents for any trajectory, including periodic orbits, in particular, not just the antisymmetric orbit. The perturbation of along the original periodic solution itself performs this role, and it is evident here that it is the only mode that can, in general. The spectrum of Lyapunov exponents should correspond to the rate of exponential growth of the perturbations with time, as discussed above. The spectrum computed independently is seen in Fig. 6 to agree with the growth rate of perturbations quantitatively.

For perturbations around symmetric orbit, at  $E/N = 100, N = 16$ , the size of the amplitudes corresponding to the modes were in descending order with respect to the modes  $m = 0, 1, \dots, N/2$ , as seen in Fig. 4. However, in the example of the antisymmetric  $E/N = 9, N = 8$ , no such simple ordering exists. It is interesting to see how the growth of perturbations, as characterized by Lyapunov exponents, depend on the mode for a given  $E/N$ . This is shown for the antisymmetric orbit for  $N = 16$  in Fig. 7, where it is seen that for large  $E/N$ , the ordering is similar to what was seen for the symmetric orbit. For perturbations around the antisymmetric orbit, the modes  $m = N/2 - 1, N/2 - 2, \dots, 2, 1, 0$  become unstable one by one as we increase  $E/N$ . However, as we increase the energy, eventually, the size of the Lyapunov exponent is in the reverse order they became non-zero. This property holds for all  $N$  we have investigated, and a mathematical structure presumably exists behind it, which still needs to be investigated.

## V. EXTENSION OF THE CONSTRUCTION AND STABILITY ANALYSIS TO MODELS WITH DIFFERENT ON-SITE POTENTIALS

As noted in Sect. III, the construction of the periodic orbits can be applied to general one dimensional lattice theories, provided the inter-site couplings are harmonic. The theory can be more general in two ways, the harmonic

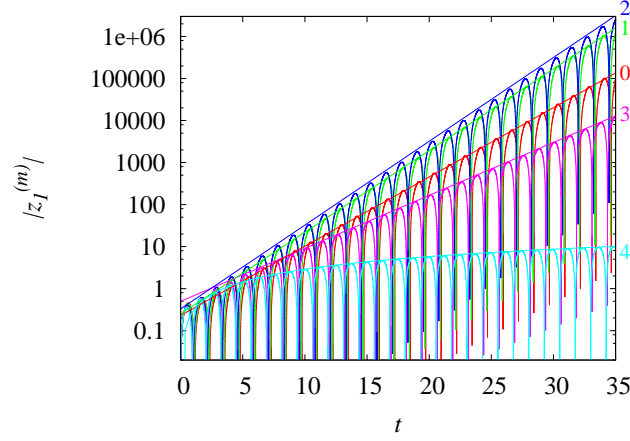


FIG. 6: Perturbation about the antisymmetric orbit for  $N = 8$ ,  $E/N = 9$ : Modes for  $m = 0$ (red), 1(green), 2(blue), 3(magenta), 4(cyan) are shown (also labeled on the right hand side), which grow exponentially with time except for mode  $m = 4$ , which grows linearly.  $\exp(\lambda^{(p)} t)$  are also shown (in color corresponding to the mode) and agree excellently with the growth of the perturbations for  $m = 0, 1, 2, 3$ . The corresponding strictly positive exponents are  $\lambda^{(0)} = 0.3795$ ,  $\lambda^{(1)} = 0.4476$ ,  $\lambda^{(2)} = 0.4591$ ,  $\lambda^{(3)} = 0.2903$  and all exponents are doubly degenerate in the Lyapunov spectrum, except for  $\lambda^{(0)}$ .  $0.29t$  is shown and agrees well with the linear growth of the perturbation for  $m = 4$ .

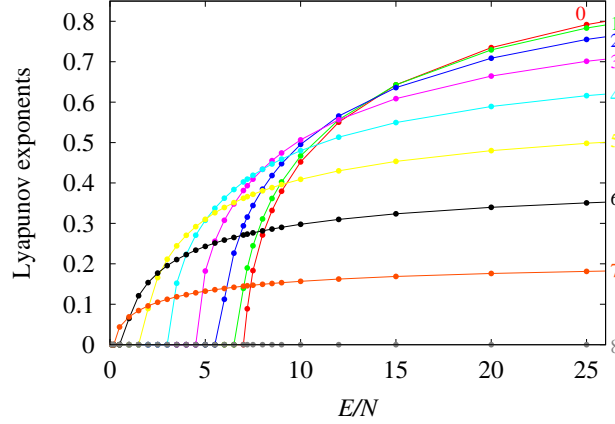


FIG. 7: The dependence on  $E/N$  of the Lyapunov exponents along the antisymmetric orbit for  $N = 16$ , corresponding to the modes  $m = 0$  (red), 1(green), 2(blue), 3(yellow), 4(cyan), 5(magenta), 6(black), 7(orange), and  $N/2=8$  (grey) (labeled in the plot). Only positive Lyapunov exponents ( $\lambda \geq 0$ ) are shown, since the negative exponents are identical, except for the sign.

part of the Hamiltonian can be different, and also, the on-site potential can be different. If the normal modes for the harmonic theory without the on-site potential, is known, we can use the condition Eq. (10) to systematically find periodic solutions. We now consider Hamiltonians without changing the inter-site potential, but with different on-site potentials,  $\Phi(q)$ . The Hamiltonian for these theories are,

$$H = \sum_{j=1}^N \frac{p_j^2}{2} + \sum_{j=1}^{N-1} \frac{(q_{j+1} - q_j)^2}{2} + H_B + \sum_{j=1}^N \Phi(q_j) \quad , \quad (24)$$

The equations of motion for the theory are coupled  $2N$  first order non-linear differential equations, in general. When a normal mode can be extended to the non-linear theory, the same construction yields the equations of motion, which is a single second order differential equation.

$$\ddot{z} = -(\omega^{(p)})^2 z - \frac{d\Phi}{dz}(z) \quad , \quad (25)$$

The condition for such a reduction to apply is identical to Eq. (10), as long as the potential is even with respect to  $z$ ,  $\Phi(-z) = \Phi(z)$ . When the potential is not even, only the symmetric mode, with all coordinates having the same value, is allowed. This mode might be incompatible with the boundary conditions of the theory. Strictly speaking, when the potential is not even, a mode with all the non-zero amplitudes having the same value is allowed, which is more general, in principle, than the symmetric mode. However, only the symmetric mode resides in this category for the Hamiltonians considered here (see, Table II). When the trajectory is bounded, it is periodic, even though the reduction of the equations of motion is applicable even when the motion is unbounded. The potential does not need to be a monomial, or even a polynomial. If the inter-site potentials are changed, the normal modes for the harmonic part will be different, but the same principle applies to extending the normal modes to the non-linear theory. We parenthetically point out one exception to these considerations, the case  $\Phi(z) = \text{const.} \times z^2$ . In this case, all the normal modes, with any amplitude, extend to the theory with this on-site potential, but the equations of motion are linear.

The perturbations around a solution,  $(q_{j,0})$ , can be analyzed analogously to the  $\phi^4$  theory. The perturbations,  $(q_{j,1})$ , satisfy

$$\ddot{q}_{j,1} = q_{j+1,1} + q_{j-1,1} - 2q_{j,1} - \frac{d^2}{dz^2}\Phi(q_{j,0})q_{j,1} \quad . \quad (26)$$

These equations are applicable in general, given any periodic solution,  $(q_{j,0})$ , obtained using Eq. (25). They can be further simplified to the following equations when  $\Phi(q_{j,0})$  is independent of  $j$ , which occurs when no zeros exist in the amplitudes of the modes, as in the  $\phi^4$  theory.

$$\ddot{z}_1^{(m)} = - \left[ \left( \omega^{(m)} \right)^2 + \frac{d^2}{dz^2}\Phi(z_0) \right] z_1^{(m)} \quad , \quad m = 0, 1, 2, \dots, N-1. \quad (27)$$

If the harmonic part of the Hamiltonian is the same as those of the coupled oscillator Eq. (1), for periodic, fixed or free boundary conditions, the general solutions to the conditions, Eq. (10), have been analyzed in Sect. III.

We now examine some concrete examples:

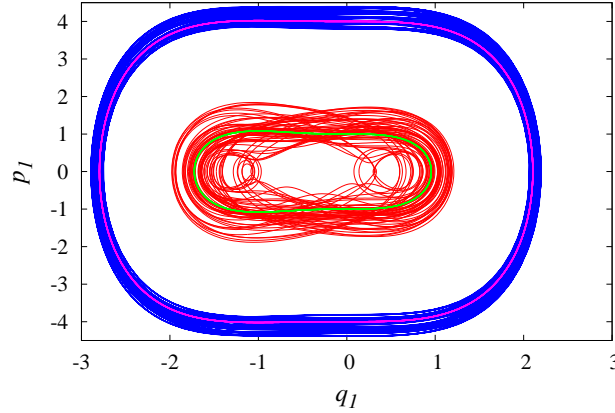


FIG. 8: Periodic orbits in phase space for the potential  $\Phi(q) = q^3/3 + q^4/4$  and their perturbations, for  $N = 4$ : The symmetric trajectory  $(q_1, p_1)$  for  $E/N = 0.5$  (green), 8 (magenta) and their perturbations (red, blue, respectively). Evidently,  $E/N = 0.5$  orbit is unstable, while  $E/N = 8$  orbit is not, which agrees with the Lyapunov spectra computed along these orbits. The orbits are not symmetric with respect to  $q_1 \leftrightarrow -q_1$  reflection and the orbits for different energies are seen to be quite dissimilar in shape. Also, the orbits both differ from the harmonic oscillator orbit, an ellipse. All trajectories were started with  $q_j = 0$  (any  $j$ ) and were followed for the same amount of time,  $\Delta t = 400$ . Perturbed orbits were obtained by increasing the initial  $p_1$  values by 10%.

*a. Cubic and quartic potential* Let us consider the example of a potential, by adding a cubic term to the quartic potential of  $\phi^4$  theory,

$$\Phi(q) = \frac{q^3}{3} + \frac{q^4}{4} \quad . \quad (28)$$

This potential is different from the  $\phi^4$  theory potential in that it is not a monomial, and further does not have the reflection symmetry  $q \leftrightarrow -q$ . Therefore, only the symmetric mode, as explained above, can be extended to the

non-linear theory, which is a solution for any  $N$ , when the boundary conditions are periodic or free. Some periodic orbits for  $N = 4$  lattice with periodic boundary conditions are shown in Fig. 8 at  $E/N = 0.5, 8$  along with their perturbed trajectories. The former is unstable and the latter is stable. There are interesting qualitative differences in the behavior, when compared to the quartic potential trajectories analyzed in the previous section. In that case, the symmetric orbit was always stable. Furthermore, when the orbit became unstable, increasing  $E/N$  only made it less stable (see Fig. 7). With the current potential, the symmetric orbit becomes unstable at lower energies and becomes stable at higher energies. This behavior might seem intuitively strange at first sight, especially since increasing the energy might naively seem to enhance the instability of the orbits. However, at higher energies, the orbit samples potentials at higher energies on average, which is governed by the quartic behavior. Therefore, the essential differences from the quartic potential case become more pronounced at lower energies. As in the previous section, the rates of growth of the perturbation modes quantitatively agree with the Lyapunov spectrum, which has been computed independently.

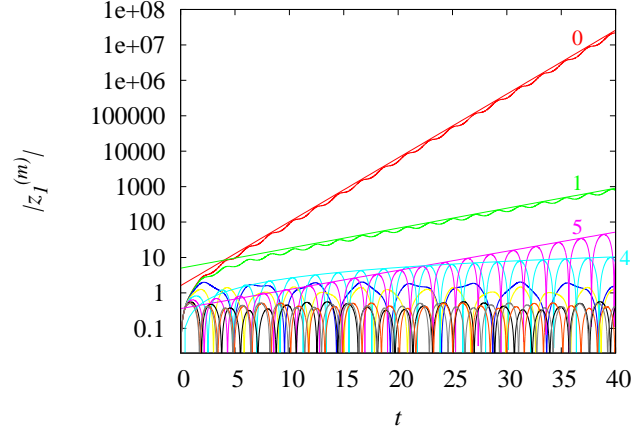


FIG. 9: Trigonometric potential: Absolute value of the perturbations,  $|z_1^{(m)}|$ , ( $m = 0, 1, \dots, N/2$ ) around the mode 2a periodic solution,  $z_0$ , with  $\omega_0^2 = 2$ , as a function of time,  $t$ , for  $N = 16$ ,  $E/N = 10$ . All the different modes  $m = 0$  (red), 1 (green), 2 (blue), 3 (yellow), 4 (cyan), 5 (magenta), 6 (black), 7 (orange),  $N/2=8$  (grey) are shown. Modes  $m = 0, 1, 5$  have exponential growing perturbations. Using the Lyapunov spectrum computed independently,  $\exp(\lambda^{(m)}t)$  corresponding to these three modes are shown, and the growth rate and the Lyapunov exponents are in excellent agreement. The corresponding exponents are  $\lambda^{(0)} = 0.4150$ ,  $\lambda^{(1)} = 0.1230$ ,  $\lambda^{(5)} = 0.1243$  and  $\lambda^{(1,5)}$  are doubly degenerate in the Lyapunov spectrum. Perturbation for mode  $m = 4$  grows linearly and its growth agrees well with  $0.34t$ , which is also shown.

*b. Trigonometric potential* As a final example, let us analyze

$$\Phi(q) = 1 - \cos(q) \quad . \quad (29)$$

This case is qualitatively different from the previous examples; the potential is *not* a polynomial function and the potential is bounded, so that there exist unbounded orbits. For this case, we analyze the perturbations around the mode based on mode 2a in Table II, for the  $N = 16$  lattice with periodic boundary conditions (Table I). This mode is different from the symmetric and the antisymmetric mode, but can be analyzed in the same fashion, using the theoretical structure introduced above.

In Fig. 9, the time dependence of the absolute values of all the perturbation modes for  $E/N = 10$  are shown. At this energy, this mode is bounded and periodic due to the quadratic part of the potential in the Hamiltonian, Eq. (24). The symmetric mode would lead to *unbounded* trajectories at the same energy. There are three unstable modes, two of which run away and will not oscillate around zero, and one unstable mode that does not run away. Such run away modes can exist when  $(\omega^{(m)})^2 < 1$  so that the time dependent frequencies in Eq. (27) can become imaginary, which corresponds to  $m/N < 1/6$ . In this example,  $m = 0, 1$  modes run away and  $m = 5$  mode has a parametric resonance type instability. These perturbations are of type (a) in Floquet's theorem with  $\alpha$  non-real. The run away solutions correspond asymptotically to periodic solutions oscillating around a non-zero value with exponentially growing amplitudes. The deviations from the simple exponential growth behavior for small  $t$  is due to the contribution of the exponentially decaying solutions.  $m = 4$  mode corresponds to the mode 2a of the unperturbed periodic solution and grows linearly, as can be seen in Fig. 9. This agrees with the general argument given at the end of Sect. IV B 1, and the solution is of type (b) in Floquet's theorem with  $\theta \neq 0$ . The Lyapunov spectrum, computed independently, confirms that there are five strictly positive exponents and their values can be seen to agree quite well

with the growth of the perturbations, as can be seen in Fig. 9. Lyapunov exponents for the  $m = 1, 5$  modes are doubly degenerate, as explained in the previous section.

## VI. DISCUSSION

In this work, we systematically constructed periodic orbits of the  $\phi^4$  theory by extending the normal modes of the harmonic limit of the model. The stability of the periodic orbits were analyzed, quantitatively relating the Lyapunov exponents to each modes. Properties of the Lyapunov spectrum, such as the degeneracy of the exponents and their relation to the harmonic spectrum were clarified. While some of the general properties have been known and explicit results have been derived for some other models[14, 15], these questions have not been studied for the  $\phi^4$  theory. We believe that the results complement the previous results in other models such as the FPU model in an interesting way, considering their different dynamical behaviors. Also, importantly, the  $\phi^4$  theory is a prototypical model in this class in various fields of physics. Furthermore, by showing how the various aspects come together explicitly, our results can hopefully serve as a concrete basis for future research. The systematic construction of the periodic orbits and their stability analysis are applicable to other models with harmonic inter-site and non-linear on-site potentials, and we studied how this can be done with models having qualitatively different behavior from the  $\phi^4$  theory. It should be noted that for this class of models, these periodic orbits exhaust the solutions in which all the coordinates move in synchronization and the overall amplitude is arbitrary, by construction. We found a fascinating consistent picture that ties together the physics of the periodic orbits, perturbation around them and the Lyapunov spectra. One can obtain Lyapunov exponents around these orbits, one  $\pm\lambda$  pair by pair, by solving a single second order differential equation at a time, rather than solving for the whole system, providing a clear picture of the system.

There are several directions to be further investigated. The  $\phi^4$  theory can be studied more deeply, using extension of normal modes and boundary conditions, other than those studied here. Also, given the general construction presented here, the dynamics of periodic orbits in models with different on-site potentials and their stability can be studied. While we have studied synchronous periodic orbits with arbitrary amplitudes for these class of theories, more general periodic solutions exist, sometimes referred to as higher dimensional bushes[20, 21]. Behavior of periodic solutions and their dependence on the properties of the on-site potential raises intriguing questions. The link between the stability and instability of the periodic orbits and the behavior of Lyapunov exponents can be studied at a deeper level. Consistency requirements and the behavior of Lyapunov exponents, as seen in Fig. 7, hint at a beautiful underlying mathematical structure, which is intriguing. We believe that the interesting subject matter studied here brings together various fields in classical dynamics; analytic aspects, such as parametric resonance, geometric aspects such as the periodic trajectories and the Lyapunov spectrum, and applied physics. We hope that the concrete results presented here for the  $\phi^4$  lattice theory and other models leads to further progress in the field.

## Acknowledgments

We would like to thank William Hoover for the collaboration that started this project, constructive comments, and encouragement. K.A. was supported in part by the Grant-in-Aid for Scientific Research (#15K05217) from the Japan Society for the Promotion of Science (JSPS), and a grant from Keio University.

- 
- [1] L.D. Landau, E.M. Lifshitz, Mechanics (3rd Edition), Pergammon Press (Oxford, 1976); H. Goldstein, C.P. Poole Jr., J.L. Safko, Classical Mechanics (3rd Edition), Pearson (Edinburgh, 2001).
  - [2] K. Aoki and D. Kusnezov, Phys. Lett. A 265, 250 (2000); K. Aoki, D. Kusnezov, Ann. Phys. 295, 50 (2002).
  - [3] B. Hu, B. Li, and H. Zhao, Phys. Rev. E 61, 3828 (2000).
  - [4] K. Aoki, D. Kusnezov, Phys. Rev. E68, 056204 (2003).
  - [5] E. Fermi, J. Pasta and S. Ulam, Collected Papers of Enrico Fermi, University of Chicago Press, Chicago (1965).
  - [6] S. Lepri, R. Livi and A. Politi, Phys. Rep. 377, 1 (2003).
  - [7] W.G. Hoover and K. Aoki, arXiv:1605.07721.
  - [8] M. Aizenman Phys. Rev. Lett. 47, 1 (1981); J. Fröhlich, Nucl. Phys. B200, 281 (1981).
  - [9] T. Degrand, D. Toussaint, From Actions to Answers, World Scientific (Singapore, 1989).
  - [10] R. Rosenberg, Adv. Appl. Mech., 9, 156 (1966).
  - [11] S.W. Shaw, C. Pierre, Journal of Sound and Vibration 150, 170 (1991), *ibid.* 164 85 (1993).
  - [12] K.W. Sandusky and J.B. Page, Phys. Rev. B 50, 866 (1994).
  - [13] S. Flach, Physica D 91, 223 (1996).

- [14] A.F. Vakakis, *Mech. Sys. Sig. Proc.* 11, 3 (1997); Y.V. Mikhlin and K.V. Avramov *Appl. Mech. Rev* 63, 060802 (2011).
- [15] T. Bountis, G. Chechin and V. Sakhnenko, *Int. J. Bif. Chaos* 21, 1539 (2011).
- [16] N. Budinsky and T. Bountis, *Physica D* 8, 445 (1983).
- [17] S. Flach, M.V. Ivanchenko and O.I. Kanakov, *Phys. Rev. Lett.* 95, 064102 (2005); *Phys. Rev. E* 73, 036618 (2006).
- [18] G.M. Chechin and D.S. Ryabov, *Phys. Rev. E* 85, 056601 (2012).
- [19] G. Kerschen, M. Peeters, J.C. Golinval, A.F. Vakakis, *Mech. Sys. Sig. Proc.* 23, 170 (2009); Konstantin V. Avramov and Yuri V. Mikhlin, *Appl. Mech. Rev* 65, 020801 (2013).
- [20] G.M. Chechin and V.P. Sakhnenko, *Physica D* 117, 43 (1998).
- [21] G.M. Chechin, G.M. Ryabov and K.G. Zhukov, *Physics D* 203, 121 (2005).
- [22] M. Tabor, *Chaos and Integrability in Nonlinear Dynamics*, John Wiley & Sons (New York, 1989).
- [23] W.G. Hoover, C.G. Hoover, *Simulation and Control of Chaotic Nonequilibrium Systems*, World Scientific Publishing Company (Singapore, 2015), and references therein.
- [24] I. Shimada, T. Nagashima, *Prog. Theor. Phys.* 61, 1605 (1979).
- [25] G. Benettin, L. Galgani, A. Giorgilli and J. Strelcyn, *Meccanica* 15, 9 (1980); *ibid.* 15, 21 (1980).
- [26] H.A. Posch, W.G. Hoover, *Phys. Rev.* A38, 473 (1988).
- [27] G.P. Morriss, *Phys. Lett.* A134, 307 (1989).
- [28] S. Sarman, D.J. Evans, and G.P. Morriss, *Phys. Rev. A* 45, 2233 (1992).
- [29] W.G. Hoover, H.A. Posch, *Phys. Rev.* E49, 1913 (1994); H.A. Posch, W.G. Hoover, *Phys. Rev.* E58, 4344 (1998).
- [30] W. Magnus and S. Winkler, *Hill's Equation*, Interscience Publishers, New York (1966).